

# Kinematics of the local Universe

## X. $H_0$ from the inverse B-band Tully-Fisher relation using diameter and magnitude limited samples

T. Ekhholm<sup>1,4</sup>, P. Teerikorpi<sup>1</sup>, G. Theureau<sup>2,3</sup>, M. Hanski<sup>1</sup>, G. Paturel<sup>4</sup>, L. Bottinelli<sup>3</sup>, and L. Gouguenheim<sup>3</sup>

<sup>1</sup> Tuorla Observatory, FIN-21500 Piikkiö, Finland

<sup>2</sup> Osservatorio Astronomico di Capodimonte, I-80 131 Napoli, Italy

<sup>3</sup> Observatoire de Paris-Meudon, CNRS URA1757, F-92195 Meudon Principal Cedex, France

<sup>4</sup> Observatoire de Lyon, F-69561 Saint-Genis Laval Cedex, France

Received 14 September 1998 / Accepted 16 April 1999

**Abstract.** We derive the value of  $H_0$  using the inverse diameter and magnitude B-band Tully-Fisher relations and the large all-sky sample KLUN (5171 spiral galaxies). Our kinematical model was that of Peebles centered at Virgo. Our calibrator sample consisted of 15 field galaxies with cepheid distance moduli measured mostly with HST. A straightforward application of the inverse relation yielded  $H_0 \approx 80 \text{ km s}^{-1} \text{ Mpc}^{-1}$  for the diameter relation and  $H_0 \approx 70 \text{ km s}^{-1} \text{ Mpc}^{-1}$  for the magnitude relation.  $H_0$  from diameters is about 50 percent and from magnitudes about 30 percent larger than the corresponding direct estimates (cf. Theureau et al. 1997b). This discrepancy could not be resolved in terms of a selection effect in  $\log V_{\text{max}}$  nor by the dependence of the zero-point on the Hubble type.

We showed that a new, calibrator selection bias (Teerikorpi et al. 1999), is present. By using samples of significant size ( $N=2142$  for diameters and  $N=1713$  for magnitudes) we found for a homogeneous distribution of galaxies ( $\alpha = 0$ ):

- $H_0 = 52_{-4}^{+5} \text{ km s}^{-1} \text{ Mpc}^{-1}$  for the inverse diameter B-band Tully-Fisher relation, and
- $H_0 = 53_{-5}^{+6} \text{ km s}^{-1} \text{ Mpc}^{-1}$  for the inverse magnitude B-band Tully-Fisher relation.

Also  $H_0$ 's from a fractal distribution of galaxies (decreasing radial number density gradient  $\alpha = 0.8$ ) agree with the direct predictions. This is the first time when the *inverse* Tully-Fisher relation clearly lends credence to small values of the Hubble constant  $H_0$  and to long cosmological distance scale consistently supported by Sandage et al. (1995).

**Key words:** galaxies: distances and redshifts – galaxies: spiral – cosmology: distance scale

### 1. Introduction

The determination of the value of the Hubble constant,  $H_0$ , is one of the classical tasks of *observational* cosmology. In the

*Send offprint requests to:* T. Ekhholm

framework of the expanding space paradigm it provides a measure of the distance scale in FRW universes and its reciprocal gives the time scale. This problem has been approached in various ways. A review on the recent determinations of the value of  $H_0$  shows that most methods provide values at  $H_0 \sim 55 \dots 75$  (for brevity we omit the units; all  $H_0$  values are in  $\text{km s}^{-1} \text{ Mpc}^{-1}$ ): Virgo cluster yields  $55 \pm 7$  and clusters from Hubble diagram with relative distances to Virgo  $57 \pm 7$  (Federspiel et al. 1998), type Ia supernovae give  $60 \pm 10$  (Branch 1998) or  $65 \pm 7$  (Riess et al. 1998), Tully-Fisher relation in I-band yields  $69 \pm 5$  (Giovanelli et al. 1997) and  $55 \pm 7$  in B-band (Theureau et al. 1997b, value and errors combined from the diameter and magnitude relations), red giant branch tip gives  $60 \pm 11$  (Salaris & Cassisi 1998), gravitational lens time delays  $64 \pm 13$  (Kundić et al. 1997) and the ‘sosies’ galaxy method  $60 \pm 10$  (Paturel et al. 1998). Sunyaev-Zeldovich effect has given lower values,  $49 \pm 29$  by Cooray (1998),  $47_{-15}^{+23}$  by Hughes & Birkinshaw (1998), but the uncertainties in these results are large due to various systematical effects (Cen, 1998). Surface brightness fluctuation studies provide a higher value of  $87 \pm 11$  (Jensen et al., 1999), but most methods seem to fit in the range 55 - 75 stated above. An important comparison to these local values may be found after the cosmic microwave background anisotropy probes (MAP and Planck) and galaxy redshift surveys (2dF and SDSS) offer us a multitude of high resolution data (Eisenstein et al., 1998). Note that most of the errors cited here as well as given in the present paper are  $1\sigma$  errors.

The present line of research has its roots in the work of Bottinelli et al. (1986), where  $H_0$  was determined using spiral galaxies in the *field*. They used the direct Tully-Fisher relation (Tully & Fisher 1977):

$$M \propto \log V_{\text{max}}, \quad (1)$$

where  $M$  is the absolute magnitude in a given band and  $\log V_{\text{max}}$  is the maximum rotational velocity measured from the hydrogen 21 cm line width of each galaxy. Gouguenheim (1969) was the

first to suggest that such a relation might exist as a distance indicator.

Bottinelli et al. (1986) paid particular attention to the elimination of the so-called *Malmquist bias*. In general terms, the determination of  $H_0$  is subject to the Malmquist bias of the 2<sup>nd</sup> kind: the inferred value of  $H_0$  depends on the distribution of the derived distances  $r$  for each true distance  $r'$  (Teerikorpi 1997). Consider the expectation value of the derived distance  $r$  at a given true distance  $r'$ :

$$E(r|r') = \int_0^{\infty} dr r P(r|r'). \quad (2)$$

The integral is done over *derived* distances  $r$ . For example, consider a strict magnitude limit: for each true distance the derived distances are exposed to an upper cut-off. Hence the expectation value for the derived distance  $r$  at  $r'$  is too small and thus  $H_0$  will be overestimated.

Observationally, the direct Tully-Fisher relation takes the form:

$$X = \text{slope} \times p + \text{cst}, \quad (3)$$

where we have adopted a shorthand  $p$  for  $\log V_{\max}$  and  $X$  denotes either the absolute magnitude  $M$  or  $\log D$ , where  $D$  labels the absolute linear size of a galaxy in kpc. In the *direct* approach the slope is determined from the linear regression of  $X$  against  $p$ . The resulting direct Tully-Fisher relation can be expressed as

$$E(X|p) = ap + b. \quad (4)$$

Consider now the *observed* average of  $X$  at each  $p$ ,  $\langle X \rangle_p$ , as a function of the true distance. The limit in  $x$  (the observational counterpart of  $X$ ) cuts off progressively more and more of the distribution function of  $X$  for a constant  $p$ . Assuming  $X = \log D$  one finds:

$$\langle X \rangle_p \geq E(X|p), \quad (5)$$

The inequality gives a practical measure of the Malmquist bias depending primarily on  $p$ ,  $r'$ ,  $\sigma_X$  and  $x_{\text{lim}}$ . The equality holds only when the  $x$ -limit cuts the luminosity function  $\Phi(X)$  insignificantly.

That the direct relation is *inevitably* biased by its nature forces one either to look for an unbiased subsample or to find an appropriate correction for the bias. The former was the strategy chosen by Bottinelli et al. (1986) where the method of normalized distances was introduced. This is the method chosen also by the KLUN project. KLUN (*Kinematics of the Local Universe*) is based on a large sample, which consists of 5171 galaxies of Hubble types T=1-8 distributed on the whole celestial sphere (cf. e.g. Paturel 1994, Theureau et al. 1997b).

Sandage (1994a, 1994b) has also studied the latter approach. By recognizing that the Malmquist bias depends not only on the imposed  $x$ -limit but also on the rotational velocities and distances, he introduced the triple-entry correction method, which has consistently predicted values of  $H_0$  supporting the long cosmological distance scale. As a practical example of this approach to the Malmquist bias cf. e.g. Federspiel et al. (1994).

Bottinelli et al. (1986) found  $H_0 = 72 \text{ km s}^{-1} \text{ Mpc}^{-1}$  using the method of normalized distances, i.e. using a sample cleaned of galaxies suffering from the Malmquist bias. This value was based on the de Vaucouleurs calibrator distances. If, instead, the Sandage-Tammann calibrator distances were used Bottinelli et al. (1986) found  $H_0 = 63 \text{ km s}^{-1} \text{ Mpc}^{-1}$  (or  $H_0 = 56 \text{ km s}^{-1} \text{ Mpc}^{-1}$  if using the old ST calibration). One appreciates the debilitating effect of the Malmquist bias by noting that when it is ignored the de Vaucouleurs calibration yields much larger values:  $H_0 \sim 100 \text{ km s}^{-1} \text{ Mpc}^{-1}$ .

Theureau et al. (1997b) by following the guidelines set out by Bottinelli et al. (1986) determined the value of  $H_0$  using the KLUN sample.  $H_0$  was determined not only using magnitudes but also diameters because the KLUN sample is constructed to be complete in angular diameters rather than magnitudes (completeness limit is estimated to be  $D_{25} = 1'.6$ ). Left with 400 unbiased galaxies (about ten times more than Bottinelli et al. (1986) were able to use) reaching up to 2000–3000  $\text{km s}^{-1}$  they found using the most recent calibration based on HST observations of extragalactic cepheids

- $H_0 = 53.4 \pm 5.0 \text{ km s}^{-1} \text{ Mpc}^{-1}$  from the magnitude relation, and
- $H_0 = 56.7 \pm 4.9 \text{ km s}^{-1} \text{ Mpc}^{-1}$  from the diameter relation.

They also discussed in their Sect. 4.2 how these results change if the older calibrations were used. For example, the de Vaucouleurs calibration would increase these values by 11%. We expect that a similar effect would be observed also in the present case.

In the present paper we ask whether the results of Theureau et al. (1997b) could be confirmed by implementing the *inverse* Tully-Fisher relation:

$$p = a'X + b', \quad (6)$$

This problem has special importance because of the “unbiased” nature that has often been ascribed to the inverse Tully-Fisher relation as a distance indicator and because of the large number of galaxies available contrary to the direct approach where one is constrained to the so called unbiased plateau (cf. Bottinelli et al. 1986; Theureau et al. 1997b). The fact that the inverse relation has its own particular biases has received increasing attention during the years (Fouqué et al. 1990, Teerikorpi 1990, Willick 1991, Teerikorpi 1993, Ekholm & Teerikorpi 1994, Freudling et al. 1995, Ekholm & Teerikorpi 1997, Teerikorpi et al. 1999 and, of course, the present paper).

## 2. Outlining the approach

As noted in the introduction the KLUN project approaches the problem of the determination of the value of  $H_0$  using field galaxies with photometric distances. Such an approach reduces to three steps

1. construction of a relative kinematical distance scale,
2. construction of a relative redshift-independent distance scale, and
3. establishment of an absolute calibration.

Below we comment on the first two steps. In particular we further develop the concept of a relevant inverse slope which may differ from the theoretical slope, but is still the slope to be used. The third step is addressed in Sect. 6. It is hoped that this review clarifies the methodological basis of the KLUN project and also makes the notation used more familiar.

### 2.1. The kinematical distance scale

The first step takes its simplest form by assuming the strictly linear Hubble law:

$$R_{\text{kin}} = V_o/H'_0 \quad (7)$$

where  $V_o$  is the radial velocity inferred from the observed redshifts and  $H'_0$  is some input value for the Hubble constant. Because  $V_o$  reflects the true kinematical distance  $R_{\text{kin}}^*$  via the true Hubble constant  $H_0^*$

$$R_{\text{kin}}^* = V_o/H_0^*, \quad (8)$$

one recognizes that Eq. 7 sets up a *relative* distance scale:

$$d_{\text{kin}} = \frac{R_{\text{kin}}}{R_{\text{kin}}^*} = \frac{H_0^*}{H'_0}. \quad (9)$$

In other words,  $\log d_{\text{kin}}$  is known next to a constant.

In a more realistic case one ought to consider also the *peculiar* velocity field. In KLUN one assumes that peculiar velocities are governed mainly by the Virgo supercluster.

In KLUN the kinematical distances are inferred from  $V_o$ 's by implementing the spherically symmetric model of Peebles (1976) valid in the linear regime. In the adopted form of this model (for the equations to be solved cf. e.g. Bottinelli et al. 1986, Ekholm 1996) the centre of the peculiar velocity field is marked by the pair of giant ellipticals M86/87 positioned at some unknown true distance  $R^*$  which is used to normalize the kinematical distance scale: the centre is at a distance  $d_{\text{kin}} = 1$ .

The required cosmological velocities  $V_{\text{cor}}$  (observed velocities corrected for peculiar motions) are calculated as

$$V_{\text{cor}} = C_1 \times d_{\text{kin}}, \quad (10)$$

where the constant  $C_1$  defines the linear recession velocity of the centre of the system assumed to be at rest with respect to the quiescent Hubble flow:

$$C_1 = V_o(\text{Vir}) + V_{\text{inf}}^{\text{LG}}. \quad (11)$$

$V_o(\text{Vir})$  is the presumed velocity of the centre and  $V_{\text{inf}}^{\text{LG}}$  is the presumed infall velocity of the Local Group into the centre of the system.

### 2.2. The redshift-independent distances

The direct Tully-Fisher relation is quite sensitive to the sampling of the luminosity function. On the other hand, when implementing the inverse Tully-Fisher relation (Eq. 6) under ideal conditions it does not matter how we sample  $X$  (Schechter 1980) in order to obtain an unbiased estimate for the inverse

parameters and, furthermore, the expectation value  $E(r|r')$  is also unbiased (Teerikorpi 1984). *However, we should sample all*  $\log V_{\text{max}}$  *for each constant true*  $X$  *in the sample*. This theoretical prerequisite is often tacitly assumed in practice. For more formal treatments on the inverse relation cf. Teerikorpi (1984, 1990, 1997) and e.g. Hendry & Simmons (1994) or Rauzy & Triay (1996).

In the inverse approach the distance indicator is

$$X = A'\langle p \rangle_X + \text{cst.}, \quad (12)$$

where  $A' = 1/a'$  following the notation adopted by Ekholm & Teerikorpi (1997; hereafter ET97). The inverse regression slope  $a'$  is expected to fulfill

$$\langle p \rangle_X \equiv E(p|X) = a'X + \text{cst.} \quad (13)$$

$\langle p \rangle_X$  is the observed average  $p$  for a given  $X$ . Eq. 13 tells that in order to find the correct  $a'$  one must sample the distribution function  $\phi_X(p)$  in such a way that  $\langle p \rangle_X = (p_o)_X$ , where  $(p_o)_X$  is the central value of the underlying distribution function.  $\phi_X(p)$  is presumed to be *symmetric* about  $(p_o)_X$  for all  $X$ . ET97 demonstrated how under these ideal conditions the derived  $\log H_0$  as a function of the kinematical distance should run horizontally as the adopted slope approaches the ideal, theoretical slope.

In practice the parameters involved are subject to uncertainties, in which case one should use instead of the unknown theoretical slope a slope which we call the *relevant* inverse slope. We would like to clarify in accurate terms the meaning of this slope which differs from the theoretical slope and which has been more heuristically discussed by Teerikorpi et al. (1999). The difference between the theoretical and the relevant slope can be expressed in the following formal way. Define the observed parameters as

$$X_o = X + \epsilon_x + \epsilon_{\text{kin}}, \quad (14)$$

$$p_o = p + \epsilon_p, \quad (15)$$

where  $X$  is inferred from  $x$  with a measurement error  $\epsilon_x$  and the kinematical distance  $d_{\text{kin}}$  has an error  $\epsilon_{\text{kin}}$  due to uncertainties in the kinematical distance scale.  $\epsilon_p$  is the observational error on  $p$ . The theoretical slope  $a'_t$  is<sup>1</sup>

$$a'_t = \frac{\text{Cov}(X, p)}{\text{Cov}(X, X)}, \quad (17)$$

while the observed slope is

$$a'_o = \frac{\text{Cov}(X_o, p_o)}{\text{Cov}(X_o, X_o)} \sim \frac{\text{Cov}(X, p) + \text{Cov}(\epsilon_x + \epsilon_{\text{kin}}, \epsilon_p)}{\text{Cov}(X, X) + \sigma_x^2 + \sigma_{\text{kin}}^2} \quad (18)$$

We call the slope  $a'_o$  relevant if it verifies for *all*  $X_o$  (Eq. 13)

$$\langle p_o \rangle_{X_o} = E(p|X_o) = a'_o X_o + \text{cst.} \quad (19)$$

<sup>1</sup> We make use of the formal definition of the slope of the linear regression of  $y$  against  $x$  with

$$\text{Cov}(x, y) = \frac{\sum(x - \langle x \rangle)(y - \langle y \rangle)}{(N - 1)}. \quad (16)$$

This definition means that the average observed value of  $p_o$  at each fixed value of  $X_o$  (derived from observations and the kinematical distance scale) is correctly predicted by Eq. 19. Note also that in the case of diameter relation,  $\epsilon_x$ ,  $\epsilon_{\text{kin}}$  and  $\epsilon_p$  are only weakly correlated. Thus the difference between the relevant slope and the theoretical slope is dominated by  $\sigma_x^2 + \sigma_{\text{kin}}^2$ . In the special case where the galaxies are in one cluster (i.e. at the same true distance), the dispersion  $\sigma_{\text{kin}}$  vanishes. In order to make the relevant slope more tangible we demonstrate in Appendix A how it indeed is the one to be used for the determination of  $H_0$ .

Finally, also selection in  $p$  and type effect may affect the derived slope making it even shallower. Theureau et al. (1997a) showed that a type effect exists seen as degenerate values of  $p$  for each constant linear diameter  $X$ . Early Hubble types rotate faster than late types. In addition, based on an observational program of 2700 galaxies with the Nançay radiotelescope, Theureau et al. (1998) warned that the detection rate in HI varies continuously from early to late types and that on average  $\sim 10\%$  of the objects remain unsuccessfully observed. Influence of such a selection, which concerns principally the extreme values of the distribution function  $\phi(p)$ , was discussed analytically by Teerikorpi et al. (1999).

### 3. A straightforward derivation of $\log H_0$

#### 3.1. The sample

KLUN sample is – according to Theureau et al. (1997b) – complete up to  $B_{\text{T}}^c = 13^{\text{m}}25$ , where  $B_{\text{T}}^c$  is the corrected total B-band magnitude and down to  $\log D_{25}^c = 1.2$ , where  $D_{25}^c$  is the corrected angular B-band diameter. The KLUN sample was subjected to exclusion of low-latitude ( $|b| \geq 15^\circ$ ) and face-on ( $\log R_{25} \geq 0.07$ ) galaxies. The centre of the spherically symmetric peculiar velocity field was positioned at  $l = 284^\circ$  and  $b = 74^\circ$ . The constant  $C_1$  needed in Eq. 10 for cosmological velocities was chosen to be  $1200 \text{ km s}^{-1}$  with  $V_o(\text{Vir}) = 980 \text{ km s}^{-1}$  and  $V_{\text{inf}}^{\text{LG}} = 220 \text{ km s}^{-1}$  (cf. Eq. 11). After the exclusion of triple-valued solutions to the Peebles' model and when the photometric completeness limits cited were imposed on the remaining sample one was left with 1713 galaxies for the magnitude sample and with 2822 galaxies for the diameter sample.

#### 3.2. The inverse slopes and calibration of zero-points

Theureau et al. (1997a) derived a common inverse diameter slope  $a' \approx 0.50$  and inverse magnitude slope  $a' \approx -0.10$  for all Hubble types considered i.e. T=1-8. These slopes were also shown to obey a simple mass-luminosity model (cf. Theureau et al. 1997a). With these estimates for the inverse slope the relation can be calibrated. At this point of derivation we ignore the effects of type-dependence and possible selection in  $\log V_{\text{max}}$ . The calibration was done by forcing the slope to the calibrator sample of 15 field galaxies with cepheid distances, mostly from

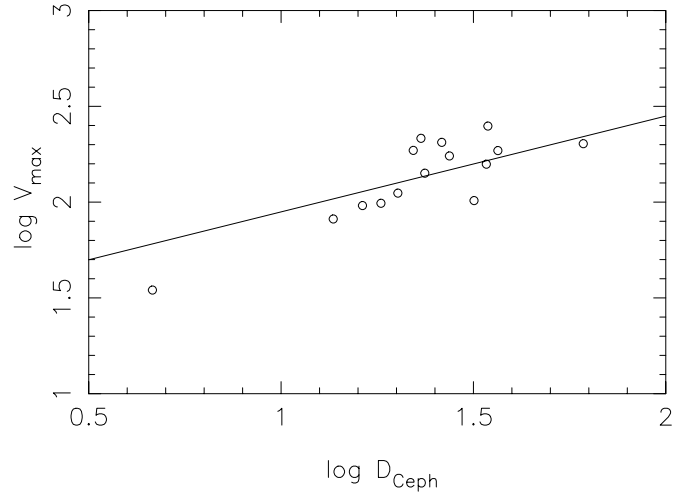


**Fig. 1.** The slope  $a' = 0.50$  forced to the calibrator sample with Cepheid distances yielding  $b'_{\text{cal}} = 1.450$ , when no type corrections were made.

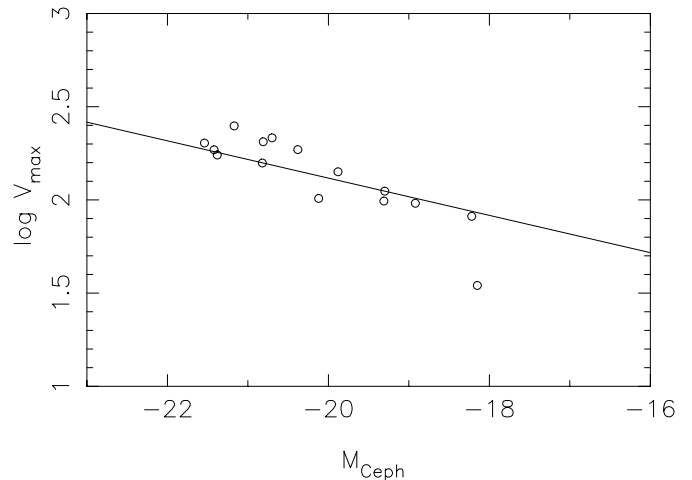


**Fig. 2.** The slope  $a' = -0.10$  forced to the calibrator sample with Cepheid distances yielding  $b'_{\text{cal}} = 0.117$ , when no type corrections were made.

the HST programs (Theureau et al. 1997b, cf. their Table 1.). The absolute zero-point is given by

$$b'_{\text{cal}} = \frac{\sum (\log V_{\text{max}} - a'X)}{N_{\text{cal}}}, \quad (20)$$

where the adopted inverse slope  $a' = 0.50$  yields  $b'_{\text{cal}} = 1.450$  and  $a' = -0.10$   $b'_{\text{cal}} = 0.117$ . In Fig. 1 we show the calibration for the diameter relation and in Fig. 2 for the magnitude relation.

#### 3.3. $H_0$ without type corrections

ET97 discussed in some detail problems which hamper the determination of the Hubble constant  $H_0$  when one applies the inverse Tully-Fisher relation. They concluded that once the relevant inverse slope is found, the average  $\langle \log H_0 \rangle$  shows no tendencies as a function of the distance. Or, in terms of the method of normalized distances of Bottinelli et al. (1986), the unbiased

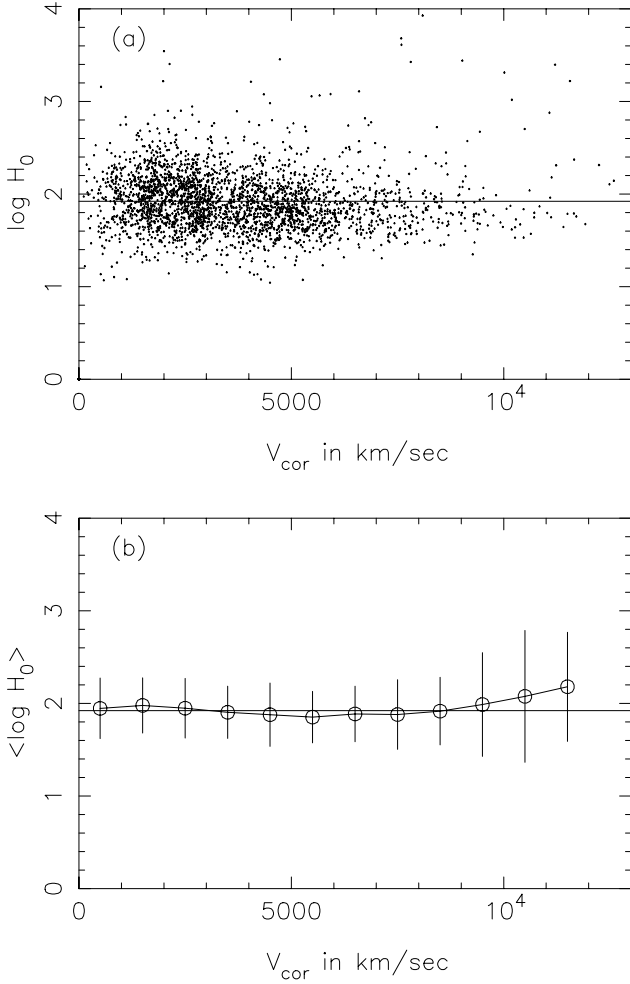


**Fig. 3a and b.** Panel (a): The  $\log H_0$  vs.  $V_{\text{cor}}$  diagram for the calibrated inverse Tully-Fisher relation  $\log V_{\text{max}} = 0.50 \log D + 1.450$ . The horizontal solid line corresponds to the average value  $\langle \log H_0 \rangle = 1.92$ . Panel (b): the average values  $\langle \log H_0 \rangle$  (circles) are shown as well as the average of the whole sample. The averages were calculated for velocity bins of size  $1000 \text{ km s}^{-1}$ . Total number of points used was  $N = 2822$ .

plateau extends to all distances. ET97 also noted how one might simultaneously fine-tune the inverse slope and get an unbiased estimate for  $\log H_0$ . The resulting  $\log H_0$  vs. kinematical distance diagrams for the inverse diameter relation is given in Fig. 3 and for the magnitude relation in Fig. 4. Application of the parameters given in the previous section yield  $\langle \log H_0 \rangle = 1.92$  corresponding to  $H_0 = 83.2 \text{ km s}^{-1} \text{ Mpc}^{-1}$  for the diameter sample and  $\langle \log H_0 \rangle = 1.857$  or  $H_0 = 71.9 \text{ km s}^{-1} \text{ Mpc}^{-1}$  for the magnitude sample. These averages are shown as horizontal, solid straight lines. In panels (a) individual points are plotted and in panels (b) the averages for bins of  $1000 \text{ km s}^{-1}$  are given as circles.

Consider first the diameter relation. One clearly sees how the average follows a horizontal line up to  $9000 \text{ km s}^{-1}$ . At larger distances, the observed behaviour of  $\langle H_0 \rangle$  probably reflects some selection in  $\log V_{\text{max}}$  in the sense that there is an upper cut-off value for  $\log V_{\text{max}}$ . Note also the mild downward

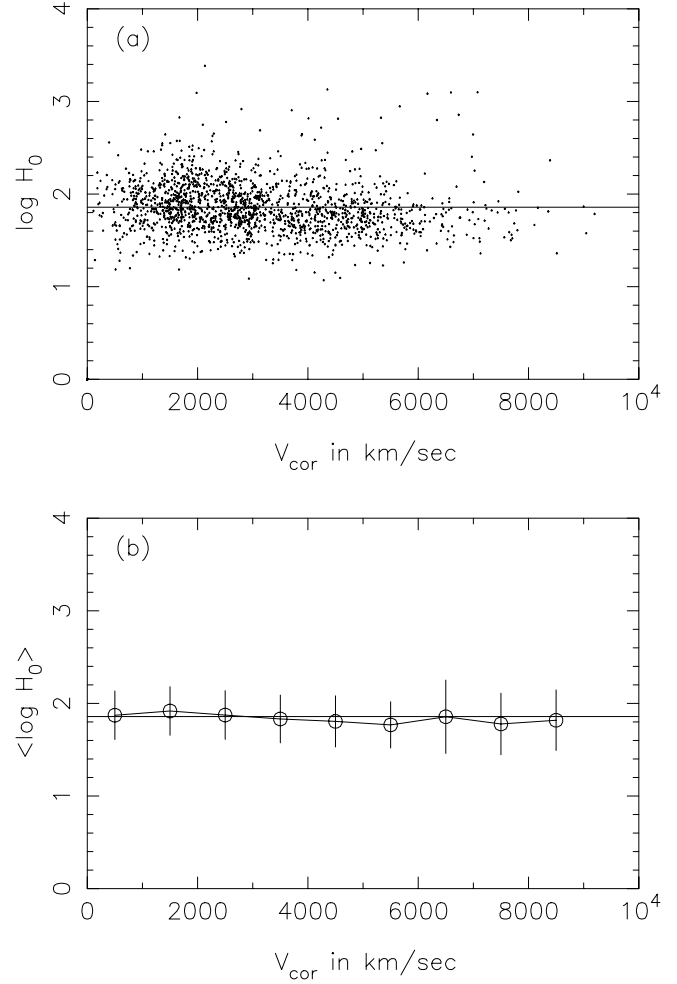


**Fig. 4a and b.** The sample imposed to the strict magnitude limit  $B_T^c = 13^m 25$  ( $N=1713$ ). The forced solution yields  $\langle \log H_0 \rangle = 1.857$  or  $H_0 = 71.9 \text{ km s}^{-1} \text{ Mpc}^{-1}$ .

tendency between  $1000 \text{ km s}^{-1}$  and  $5000 \text{ km s}^{-1}$ . Comparison of Fig. 4 with Fig. 3 shows how  $\langle \log H_0 \rangle$  from magnitudes and diameters follow each other quite well as expected (ignoring, of course, the vertical shift in the averages). Note how the growing tendency of  $\langle \log H_0 \rangle$  beyond  $9000 \text{ km s}^{-1}$  is absent in the magnitude sample because of the limiting magnitude: the sample is less deep. This suggests that the possible selection bias in  $\log V_{\text{max}}$  does not affect the magnitude sample.

One might, by the face-value, be content with the slopes adopted as well as with the derived value of  $H_0$ . The observed behaviour is what ET97 argued to be the prerequisite for an unbiased estimate for the Hubble constant: non-horizontal trends disappear. It is – however – rather disturbing to note that the values of  $H_0$  obtained via this straightforward application of the inverse relation are significantly *larger* than those reported by Theureau et al. (1997b). The inverse diameter relation predicts some 50 percent larger value and the magnitude relation some 30 percent larger value than the corresponding direct relations. In what follows, we try to understand this discrepancy.

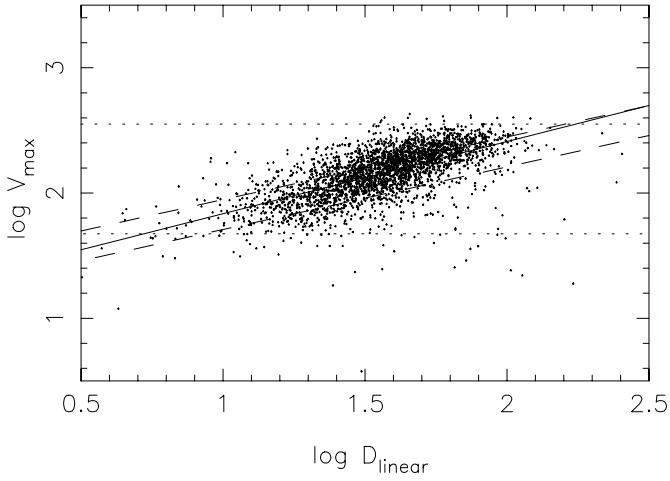


**Fig. 5.** The inverse Tully-Fisher diagram for the sample used in the analysis. The solid line refers to a linear regression of  $a' = 0.576$  and  $b' = 1.256$ . The dashed lines give the forced solutions with  $a' = 0.50$  for Hubble types 1 with  $b' = 1.448$  and 8 with  $b' = 1.209$ . The dotted lines at  $\log V_{\max} = 2.55$  and  $\log V_{\max} = 1.675$  are intended to guide the eye. At least the upper cut-off is quite conspicuous.

#### 4. Is there selection in $\log V_{\max}$ ?

The first explanation coming to mind is that the apparently well-behaving slope  $a' = 0.5$  ( $a' = -0.1$ ) is incorrect because of some selection effect and is thus *not* relevant in the sense discussed in Sect. 2.2 and in Appendix A. The relevant slope brings about an unbiased estimate for the Hubble parameter (or the Hubble constant if one possesses an ideal calibrator sample) *if* the distribution function of  $\log V_{\max}$ ,  $\phi(p)_X$ , is completely and correctly sampled for each  $X$ . Fig. 3 showed some preliminary indications that this may not be the case as regards the diameter sample.

Teerikorpi (1999) discussed the effect and significance of a strict upper and/or lower cut-off on  $\phi(p)_X$ . For example, an upper cut-off in  $\phi(p)_X$  should yield a too large value of  $H_0$  and, furthermore, a too shallow slope. Their analytical calculations given the gaussianity of  $\phi(p)_X$  show that this kind of selection effect has only a minuscule affect unless the cut-offs are considerable. Because the selection does not seem to be significant, we do not expect much improvement in  $H_0$ .

There is, however, another effect which may alter the slope. As mentioned in Sect. 2.2 the type-dependence of the zero-point should be taken into account. Because the selection function may depend on the morphological type it also affects the type corrections. This is clearly seen when one considers how the type corrections are actually calculated. As in Theureau et al. (1997b) galaxies are shifted to a common Hubble type 6 by applying a correction term  $\Delta b' = b'(T) - b'(6)$  to individual  $\log V_{\max}$  values, where

$$b'(T) = \langle \log V_{\max} \rangle_T - a' \langle X \rangle_T. \quad (21)$$

Different morphological types do not have identical spatial occupation, which is shown in Fig. 5 for Hubble types 1 and 8 as dashed lines corresponding to forced solutions using the com-

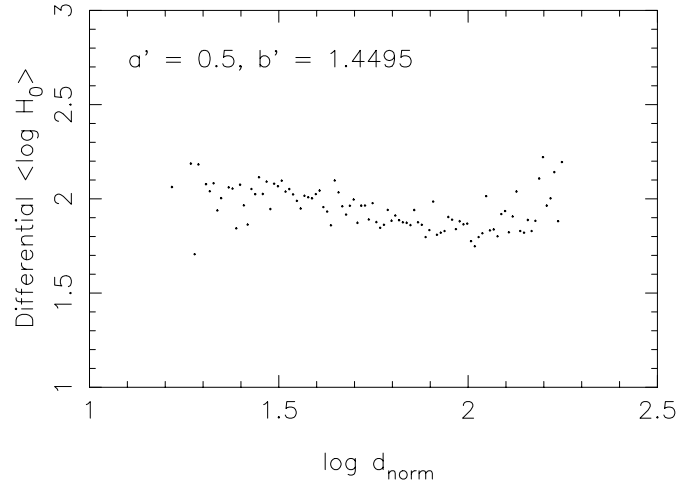


**Fig. 6.** The differential behaviour of  $\langle \log H_0 \rangle$  as a function of the normalized distances. The inverse parameters were  $a' = 0.5$  and  $b' = 1.450$ .

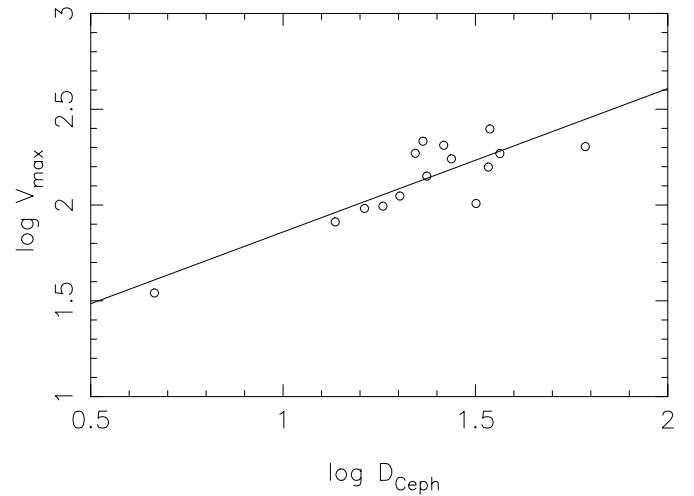


**Fig. 7.** A straightforward linear regression applied to the calibrator sample yielding  $a' = 0.749$  and  $b' = 1.101$ .

mon slope  $a' = 0.5$ . The strict upper and lower cut-offs would influence the extreme types more. Hence we must first more carefully see if the samples suffer from selection in  $\log V_{\max}$ .

The inverse Tully-Fisher diagram for the diameter sample is given in Fig. 5. The least squares fit ( $a' = 0.576$ ,  $b' = 1.259$ ) is shown as a solid line. One finds evidence for both an upper and lower cut-off in the  $\log V_{\max}$ -distribution, the former being quite conspicuous. The dotted lines are positioned at  $\log V_{\max} = 2.55$  and  $\log V_{\max} = 1.675$  to guide the eye. Fig. 5 hints that the slope  $a' = 0.5$  adopted in Sect. 3 may not be impeccable and thus questions the validity of the “naïve” derivation of  $H_0$  at least in the case of the diameter sample.

In the case of diameter samples, Teerikorpi et al. (1999) discussed how the cut-offs should demonstrate themselves in a  $\log H_0$  vs.  $\log d_{\text{norm}}$  diagram, where  $\log d_{\text{norm}} = \log D_{25} + \log d_{\text{kin}}$ , which in fact is the log of  $D_{\text{linear}}$  next to a constant. We call  $d_{\text{norm}}$  “normalized” in analogy to the method of normalized

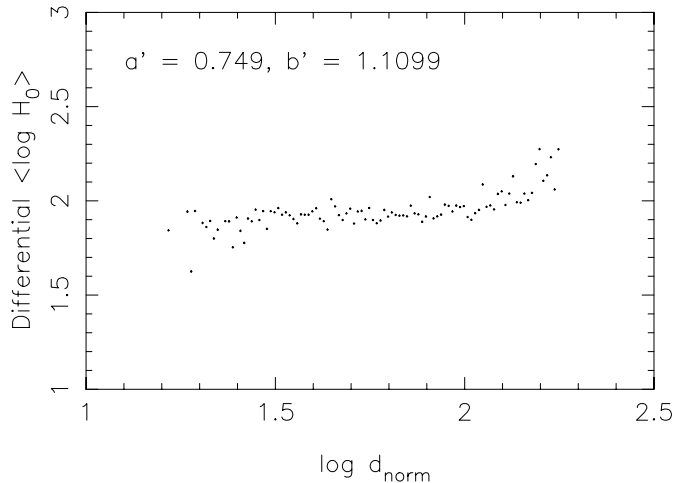


**Fig. 8.** As Fig. 6, but now the parameters  $a' = 0.749$  and  $b' = 1.101$  were used. One can see how the downward tendency between  $\log d_{\text{norm}} \sim 1.45$  and  $\log d_{\text{norm}} \sim 2$  has disappeared. Also cf. Fig. 2 in Teerikorpi et al. (1999).

distances, where the kinematical distances were normalized in order to reveal the underlying bias. That is exactly what is done also here.

Consider the differential behaviour of  $\langle \log H_0 \rangle$  as a function of the normalized distance. Differential average  $\langle \log H_0 \rangle$  was calculated as follows. The abscissa was divided into intervals of 0.01 starting at minimum  $\log d_{\text{norm}}$  in the sample. If a bin contained at least 5 galaxies the average was calculated. In Fig. 6. the inverse parameters  $a' = 0.5$  and  $b' = 1.450$  were used. It is seen that around  $\log d_n \sim 2$  the values of  $\log H_0$  have a turning point as well as at  $\log d_n \sim 1.45$ . The most striking feature is – however – the general decreasing tendency of  $\log H_0$  between these two points. Now, according to ET97, a downward tendency of  $\log H_0$  as a function of distance corresponds to  $A/A' > 1$ , i.e. the adopted slope  $A$  is too shallow ( $A'$  is the relevant slope).

Closer inspection of Fig. 1 shows that a steeper slope might provide a better fit to the calibrator sample. One is thus tempted to ask what happens if one adopts for the field sample the slope giving the best fit to the calibrator sample. As such solution we adopt the straightforward linear regression yielding  $a' = 0.749$  and  $b' = 1.101$  shown in Fig. 7. It is interesting to note that when these parameters are used the downward tendency between  $\log d_{\text{norm}} \sim 1.45$  and  $\log d_{\text{norm}} \sim 2$  disappears as can be seen in Fig. 8. From hereon we refer to this interval as the “unbiased inverse plateau”. The value of  $\log H_0$  in this plateau is still rather high.

In the case of the magnitude sample we study the behaviour of the differential average  $\langle \log H_0 \rangle$  as a function of a “normalized” distance modulus:

$$\mu_{\text{norm}} = B_T^c - 5 \log d_{\text{kin}}. \quad (22)$$

The  $\mu_{\text{norm}}$  axis was divided into intervals of 0.05 and again, if in a bin is more than five points the average is calculated. As suspected in the view of Fig. 4., Fig. 9 reveals no significant

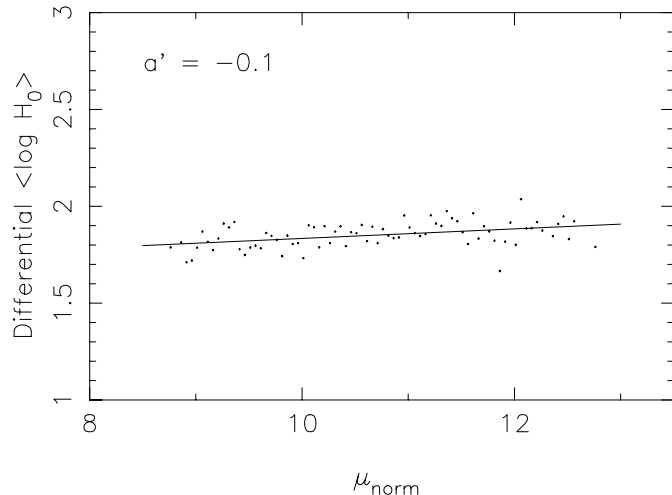


**Fig. 9.** The differential  $\langle \log H_0 \rangle$  vs.  $\mu_{\text{norm}}$  diagram. One finds no indication of a selection in  $\log V_{\text{max}}$ . The adopted slope ( $a' = -0.10$ ) appears to be incorrect.

indications of a selection in  $\log V_{\text{max}}$ . The points follow quite well the straight line also shown. The line however is tilted telling us that the input slope  $a' = -0.10$  may not be the relevant one.

As already noted the type corrections may have some influence on the slopes. In the next section we derive the appropriate type corrections for the zero-points using galaxies residing in the unbiased plateau ( $\log d_{\text{norm}} \in [1.45, 2.0]$ ) for the diameter sample and for the whole magnitude sample and rederive the slopes.

## 5. Type corrections and the value of $H_0$

The zero-points needed for the type corrections are calculated using Eq. 21. It was pointed out in Sect. 2.2 that  $\log H_0$  should run horizontally in order to find an unbiased estimate for  $H_0$ . In this section we look for such a slope. Because the type-corrections depend on the adopted slope, this fine-tuning of the slope must be carried out in an iterative manner. This process consists of finding the type corrections  $\Delta b'(T)$  for each test slope  $a'$ . Corrections are made for both the field and calibrator samples. The process is repeated until a horizontal  $\langle \log H_0 \rangle$  run is found.

Consider first the diameter sample. When the criteria for the unbiased inverse plateau were imposed on the sample, 2142 galaxies were left. For this subsample the iteration yielded  $a' = 0.54$  (the straight line in Fig. 10 is the least squares fit with a slope 0.003) and when the corresponding type corrections given in Table 1 were applied to the calibrator sample and the slope forced to it one found  $b'_{\text{cal}}(6) = 1.325$ . The result is shown in Fig. 10. The given inverse parameters predict an average  $\langle \log H_0 \rangle = 1.897$  (or  $H_0 = 78.9 \text{ km s}^{-1} \text{ Mpc}^{-1}$ ).

We treated the magnitude sample of 1713 galaxies in a similar fashion. The resulting best fit is shown in Fig. 11. The relevant slope is  $a' = -0.115$  (the least squares fit yields a slope 0.0004). The corresponding type corrections are given

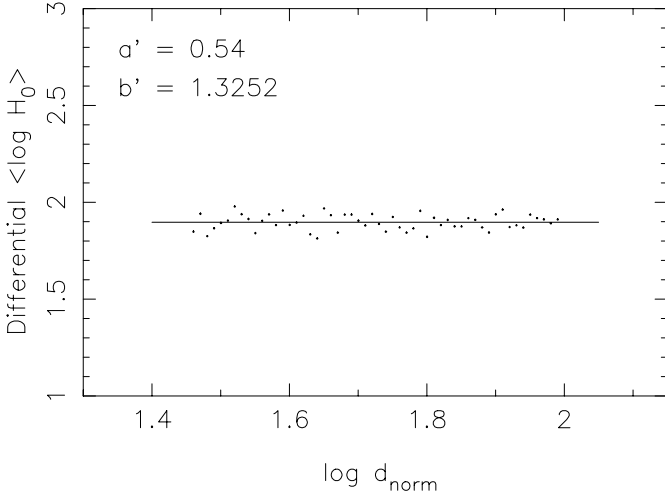


**Fig. 10.** The differential  $\langle \log H_0 \rangle$  as a function of the log of normalized distance  $\log d_{\text{norm}}$  for the plateau galaxies with the adopted relation  $\log V_{\text{max}} = 0.54 \log D + 1.325$ . The solid line is the average  $\log H_0 = 1.897$ .

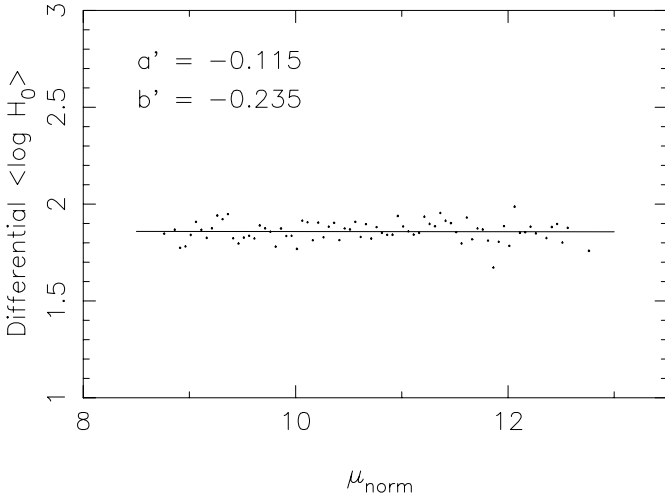


**Fig. 11.** The differential  $\langle \log H_0 \rangle$  as a function of the log of normalized distance modulus  $\mu_{\text{norm}}$  for the plateau galaxies with the adopted relation  $\log V_{\text{max}} = -0.115M - 0.235$ . The solid line is the average  $\log H_0 = 1.869$ .

in Table 1. The forced calibration gives  $b'_{\text{cal}}(6) = -0.235$ . From this sample we find an average  $\langle \log H_0 \rangle = 1.869$  (or  $H_0 = 72.4 \text{ km s}^{-1} \text{ Mpc}^{-1}$ ). In both cases the inverse estimates for the Hubble constant ( $H_0 \approx 80$  for the diameter relation and  $H_0 \approx 70$  for the magnitude relation) are considerably larger than the corresponding estimates using the direct Tully-Fisher relation ( $H_0 \approx 55$ ).

## 6. $H_0$ corrected for a calibrator selection bias

The values of  $H_0$  from the direct and inverse relations still disagree *even* after we have taken into account the selection in  $\log V_{\text{max}}$ , made the type corrections and used the relevant slope. There is – however – a serious possibility left to explain the dis-

**Table 1.** The type corrections required for the relevant slopes  $a' = 0.54$  for the unbiased diameter sample and  $a' = -0.115$  for the magnitude sample.

$\Delta b'(T)$	$a' = 0.54$	$a' = -0.115$
$\Delta b'(1)$	0.125	0.110
$\Delta b'(2)$	0.156	0.124
$\Delta b'(3)$	0.129	0.096
$\Delta b'(4)$	0.095	0.058
$\Delta b'(5)$	0.069	0.030
$\Delta b'(6)$	0.0	0.0
$\Delta b'(7)$	-0.054	-0.042
$\Delta b'(8)$	-0.118	-0.075

crepancy. *The calibrator sample used may not meet the theoretical requirements of the inverse relation.* In order to transform the relative distance scale into an absolute one a properly chosen sample of calibrating galaxies is needed. What does “properly chosen” mean? Consider first the direct relation for which it is essential to possess a calibrator sample, which is volume-limited for *each*  $p_{\text{cal}}$ . This means that for a  $p_{\text{cal}}$  one has  $X_{\text{cal}}$  which is drawn from the complete part of the gaussian distribution function  $G(X; X_p, \sigma_{X_p})$ , where the average  $X_p = ap + b$ . If  $\sigma_{X_p}$  is constant for all  $p$  and the direct slope  $a$  has been *correctly* derived from the unbiased field sample, it will, when forced onto the calibrator sample, bring about the correct calibrating zero-point.

As regards the calibration of the inverse relation the sample mentioned above does not necessarily guarantee a successful calibration. As pointed out by Teerikorpi et al. (1999) though the calibrator sample is complete in the *direct* sense nothing has been said about how the  $p_{\text{cal}}$ ’s relate to the corresponding cosmic distribution of  $p$ ’s from which the field sample was drawn.  $\langle p \rangle_{\text{cal}}$  should reflect the cosmic average  $p_0$ . If not, the relevant field slope when forced to the calibrator sample will bring about a biased estimate for  $H_0$ . Teerikorpi (1990) already recognized that this could be a serious problem. He studied, however, clusters of galaxies where a nearby (calibrator) cluster obeys a different slope than a distant cluster. Teerikorpi et al. (1999) developed the ideas further and showed how this problem may be met also when using field galaxies. The mentioned bias when using the relevant slope can be corrected for but is a rather complicated task. For the theoretical background of the “calibrator selection bias” consult Teerikorpi et al. (1999).

One may – as pointed out by Teerikorpi et al. (1999) – use instead of the relevant slope the calibrator slope which also predicts a biased estimate for  $H_0$  but which can be corrected for in a rather straightforward manner. For the diameter relation the average correction term reads as

$$\Delta \log H_0 = (3 - \alpha) \ln 10 \sigma_D^2 \times \left[ \frac{a'_{\text{cal}}}{a'} - 1 \right], \quad (23)$$

where  $\sigma_D$  is the dispersion of the log linear diameter  $\log D_{\text{linear}}$  and  $\alpha$  gives the radial number density gradient:  $\alpha = 0$  corresponds to a strictly homogeneous distribution of galaxies. For

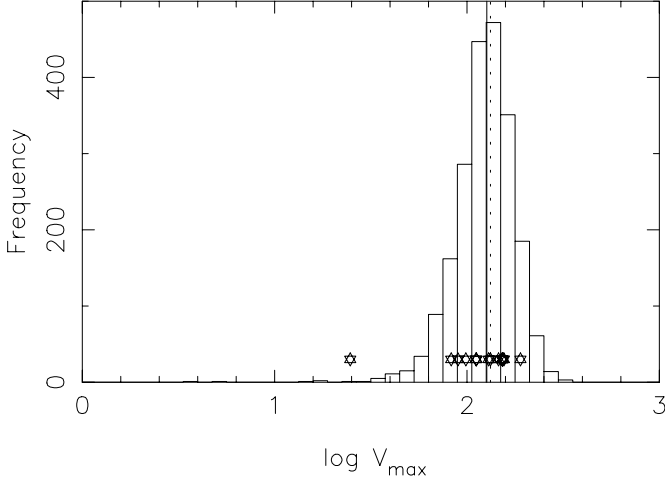


**Fig. 12.** Histogram of the  $\log V_{\max}$  values and the individual calibrators (labelled with stars). The vertical solid line gives the median of the plateau  $\text{Med}(\log V_{\max}^{\text{plateau}}) = 2.10$  and the dotted line gives the median of the calibrators  $\text{Med}(\log V_{\max}^{\text{calib}}) = 2.11$ .

magnitudes the correction term follows from (cf. Teerikorpi 1990)

$$\Delta \log H_0 = 0.2 \left[ \frac{a'_{\text{cal}}}{a'} - 1 \right] \times (\langle M \rangle - M_0). \quad (24)$$

Because  $\langle M \rangle - M_0$  simply reflects the classical Malmquist bias one finds:

$$\Delta \log H_0 = \frac{(3 - \alpha) \ln 10}{5} \sigma_M^2 \times 0.2 \left[ \frac{a'_{\text{cal}}}{a'} - 1 \right], \quad (25)$$

Note that one may use the calibrator slope and consequently the correction formulas *irrespective* of the nature of the calibrator sample (Teerikorpi et al. 1999). If the calibrator sample would meet the requirement mentioned, the value corrected with Eqs. 23 or 25 should equal values obtained from the relevant slopes. Furthermore, our analysis carried out so far would have yielded an unbiased estimate for  $H_0$  and thus the problems would be in the direct analysis. However, if the requirement is not met one should prefer the corrective method using the calibrator slope.

### 6.1. Is the calibrator sample representative?

Is the calibrator bias present in our case? Recall that the calibrators used were sampled from the nearby field to have high quality distance moduli mostly from the HST Cepheid measurements. This means that we have no a priori guarantee that the calibrator sample used will meet the criterium required. We compare the type-corrected diameter and magnitude samples with the calibrator sample. Note that for the diameter sample we use only galaxies residing in the unbiased inverse plateau (i.e. the small selection effect in  $\log V_{\max}$  has been eliminated). In Fig. 12 we show the histogram of the  $\log V_{\max}$  values for the diameter sample and the individual calibrators (labelled as stars). The vertical solid line gives the median of the plateau

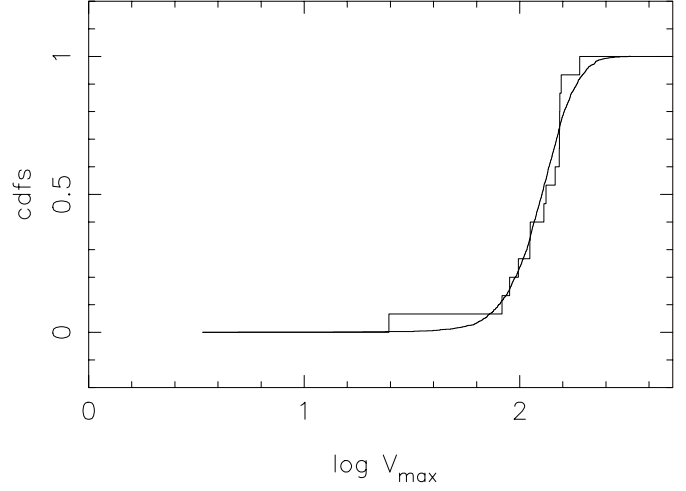


**Fig. 13.** The Kolmogorov-Smirnov test for the diameter sample. Pay attention to the rather remarkable similarity between the cumulative distribution functions (cdfs).

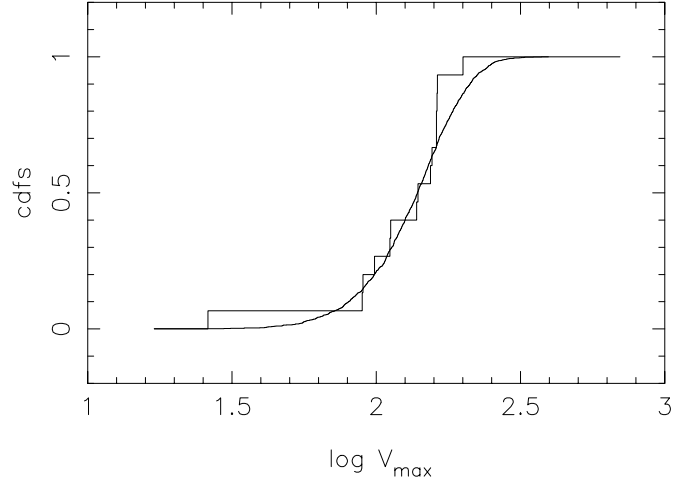


**Fig. 14.** The Kolmogorov-Smirnov test for the magnitude sample. Again the cdfs are quite similar.

$\text{Med}(\log V_{\max}^{\text{plateau}}) = 2.10$  and the dotted line gives the median of the calibrators  $\text{Med}(\log V_{\max}^{\text{calib}}) = 2.11$ . In the case of magnitudes both the field and calibrator sample have the same median (2.14). The average values for the diameter case were  $\langle \log V_{\max}^{\text{plateau}} \rangle = 2.09$  and  $\langle \log V_{\max}^{\text{calib}} \rangle = 2.06$ , and for the magnitude case  $\langle \log V_{\max}^{\text{mag}} \rangle = 2.12$  and  $\langle \log V_{\max}^{\text{calib}} \rangle = 2.08$ . Both the diameter and the magnitude field samples were subjected to strict limits, which means that both inevitably suffer from the classical Malmquist bias. In order to have a representative calibrator sample in the sense described, we would have expected a clear difference between the field and calibrator samples. That the statistics are very close to each other lends credence to the assumption that the calibrator selection bias is present.

We also made tests using the Kolmogorov-Smirnov statistics (Figs. 13 and 14). In this test a low significance level should be considered as counterevidence for a hypothesis that two samples

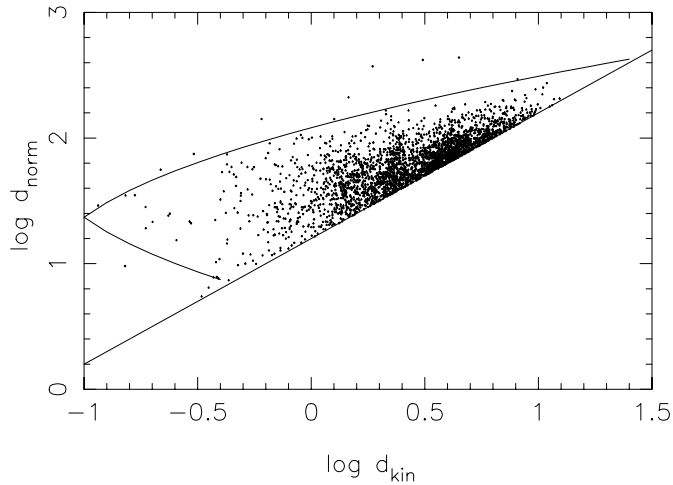


**Fig. 15.** A classical Spaenhauer diagram for normalized distances vs. kinematical distances with a presumed dispersion  $\sigma_X = 0.28$ .

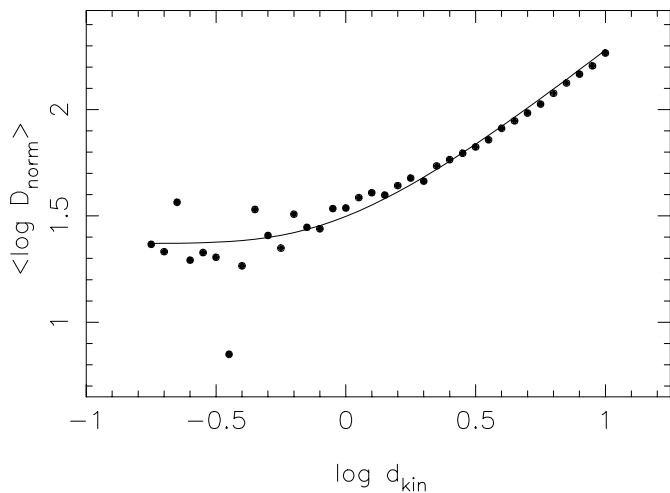


**Fig. 16.** Comparison between average values of  $\langle \log d_{\text{norm}} \rangle$  for different kinematical distances and the theoretical prediction calculated from Eq. 26 with  $X_0^* = 1.37$  and  $\sigma_X = 0.28$ .

rise from the same underlying distribution. We found relatively high significance levels (0.89 for the diameter sample and 0.3 for the magnitude sample). Neither these findings corroborate the hypothesis that the calibrator sample is drawn from the cosmic distribution and hence the use of Eqs. 23 or 25 is warranted.

### 6.2. The dispersion in $\log D_{\text{linear}}$

In order to find a working value for the dispersion in  $\log D_{\text{linear}}$ , we first consider the classical Spaenhauer diagram (cf. Sandage 1994a, 1994b). In the Spaenhauer diagram one studies the behaviour of  $X$  as a function of the redshift. If the observed redshift could be translated into the corresponding cosmological distance, then  $X$  inferred from  $x$  and the redshift would genuinely reflect the true size of a galaxy.

In practice, the observed redshift cannot be considered as a direct indicator of the cosmological distance because of the

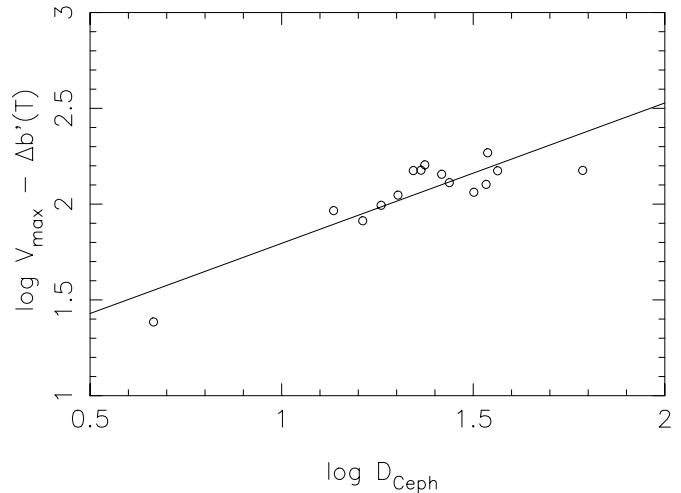


**Fig. 17.** A least squares fit to the type corrected calibrator sample yielding  $a' = 0.73$ . The type correction was based on  $a' = 0.54$ .

inhomogeneity of the Local Universe. Peculiar motions should also be considered. Thus the inferred  $X$  suffers from uncertainties in the underlying kinematical model. The Spaenhauer diagram as a diagnostics for the distribution function is always constrained by our knowledge of the form of the true velocity-distance law.

Because the normalized distance (cf. Sect. 3.) is proportional to the linear diameter we construct the Spaenhauer diagram as  $\log d_{\text{norm}}$  vs.  $\log d_{\text{kin}}$  thus avoiding the uncertainties in the absolute distance scale. The problems with relative distance scale are – of course – still present. The fit shown in Fig. 15 is not unacceptable. The dispersion used was  $\sigma_X = 0.28$ , a value inferred from the dispersion in absolute B-band magnitudes  $\sigma_M = 1.4$  (Fouqué et al. 1990) based on the expectation that the dispersion in  $\log$  linear diameter should be one fifth of that of absolute magnitudes.

We also looked how the average values  $\langle \log d_{\text{norm}} \rangle$  at different kinematical distances compare to the theoretical prediction which, in a strictly limited sample of  $X$ 's, at each  $\log$  distance is formally expressed as

$$\langle X \rangle_d = X_0^* + \frac{2\sigma_X \exp[-(X_{\text{lim}} - X_0^*)^2 / (2\sigma_X^2)]}{\sqrt{2\pi} \operatorname{erfc}[(X_{\text{lim}} - X_0^*) / (\sqrt{2}\sigma_X)]}. \quad (26)$$

Here  $X$  refers to  $\log d_{\text{norm}}$ . The curve in Fig. 16 is based on  $X_0^* = 1.37$  and  $\sigma_X = 0.28$ . The averages from the data are shown as bullets. The data points follow the theoretical prediction reasonably well.

### 6.3. Corrections and the value of $H_0$

Consider a strictly homogeneous universe, i.e.  $\alpha = 0$ . In Eqs. 23 and 25 one needs values for slope  $a'_c$ . Least squares fit to the type-corrected calibrator sample yields  $a'_c = 0.73$  for the diameter relation and  $a'_c = -0.147$  for the magnitude relation. (cf. Figs. 17 and 18). These slopes correspond to diameter zero-point  $b'_c(6) = 1.066 \pm 0.103$  and to magnitude zero-

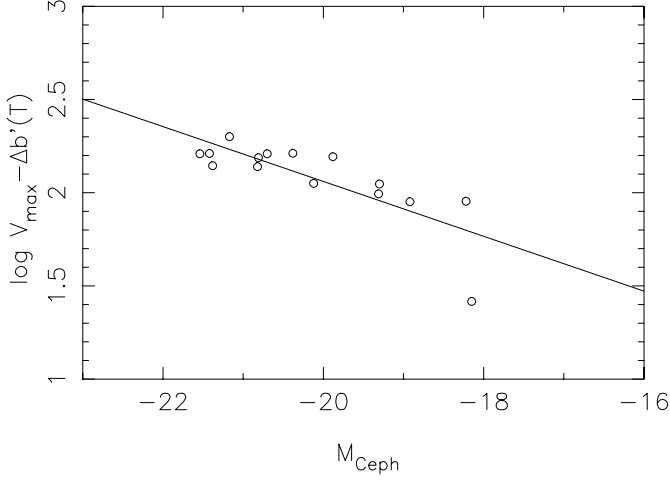


**Fig. 18.** A least squares fit the type corrected calibrator sample yielding  $a' = -0.147$ . The type correction was based on  $a' = -0.115$ .

point  $b'_c = -0.879 \pm 0.131$ . The *biased* estimates for average  $\log H_0$  are  $\langle \log H_0 \rangle = 1.910 \pm 0.188$  for the diameters and  $\langle \log H_0 \rangle = 1.876 \pm 0.176$  for the magnitudes. For the zero-points and the averages we have given the  $1\sigma$  standard deviations. The *mean error* in the averages is estimated from

$$\epsilon_{\langle \log H_0 \rangle} \approx \sqrt{\frac{\sigma_{B'}^2}{N_{\text{cal}}} + \frac{\sigma_{\log H_0}^2}{N_{\text{gal}}}}, \quad (27)$$

where  $\sigma_{B'} = \sigma_{b'}/a'_{\text{cal}}$  for diameters and  $\sigma_{B'} = 0.2\sigma_{b'}/a'_{\text{cal}}$  for magnitudes. The use of Eq. 27 is acceptable because the dispersion in  $b'$  does not correlate with the dispersion  $\log H_0$ . With the given slopes and dispersions we find:

- $\langle \log H_0 \rangle = 1.910 \pm 0.037$  for the diameters
- $\langle \log H_0 \rangle = 1.876 \pm 0.046$  for the magnitudes.

Eq. 23 predicts an average correction term for the slopes  $a'_c = 0.73$  and  $a' = 0.54$  together with  $\sigma_X = 0.28$   $\Delta \log H_0 = 0.191$ , and Eq. 25 with  $a'_c = -0.147$ ,  $a' = -0.115$  and  $\sigma_M = 1.4$   $\Delta \log H_0 = 0.151$ . When applied to the above values we get the corrected, unbiased estimates

- $\langle \log H_0 \rangle = 1.719 \pm 0.037$  for the diameters
- $\langle \log H_0 \rangle = 1.725 \pm 0.046$  for the magnitudes.

These values translate into Hubble constants

- $H_0 = 52^{+5}_{-4} \text{ km s}^{-1} \text{ Mpc}^{-1}$  for the inverse diameter B-band Tully-Fisher relation, and
- $H_0 = 53^{+6}_{-5} \text{ km s}^{-1} \text{ Mpc}^{-1}$  for the inverse magnitude B-band Tully-Fisher relation.

These corrected values are in good concordance with each other as well as with the estimates established from the direct diameter Tully-Fisher relation (Theureau et al. 1997b). Note that the errors in the magnitude relation are slightly larger than in the diameter relation. This is expected because for the diameter relation we possess more galaxies. The error is however mainly governed by the uncertainty in the calibrated zero-point. This

is expected because though the dispersion in inverse relation as such is large it is compensated by the number galaxies available.

Finally, how significant an error do the correction formulae induce? We suspect the error to mainly depend on  $\alpha$ . The correction above was based on the assumption of homogeneity (i.e.  $\alpha = 0$ ). Recently Teerikorpi et al. (1998) found evidence that the average density radially decreases around us ( $\alpha \approx 0.8$ ) confirming the more general (fractal) analysis by Di Nella et al. (1996). Using this value of  $\alpha$  we find  $\Delta \log H_0 = 0.140$  for the diameters and  $\Delta \log H_0 = 0.111$  for the magnitudes yielding

- $\langle \log H_0 \rangle = 1.770 \pm 0.037$  for the diameters
- $\langle \log H_0 \rangle = 1.765 \pm 0.046$  for the magnitudes.

In terms of the Hubble constant we find

- $H_0 = 59^{+5}_{-4} \text{ km s}^{-1} \text{ Mpc}^{-1}$  for the inverse diameter B-band Tully-Fisher relation, and
- $H_0 = 58^{+6}_{-5} \text{ km s}^{-1} \text{ Mpc}^{-1}$  for the inverse magnitude B-band Tully-Fisher relation.

## 7. Summary

In the present paper we have examined how to apply the inverse Tully-Fisher relation to the problem of determining the value of the Hubble constant,  $H_0$ , in the practical context of the large galaxy sample KLUN. We found out that the implementation of the inverse relation is not as simple task as one might expect from the general considerations (in particular the quite famous result of the unbiased nature of the relation). We summarize our main results as follows.

1. A straightforward application of the inverse relation consists of finding the average Hubble ratio for each kinematical distance and transforming the relative distance into an absolute one through calibration. The 15 calibrator galaxies used were drawn from the field with cepheid distance moduli obtained mostly from the HST observations. The inverse diameter relation predicted  $H_0 \approx 80 \text{ km s}^{-1} \text{ Mpc}^{-1}$  and the magnitude relation predicted  $H_0 \approx 70 \text{ km s}^{-1} \text{ Mpc}^{-1}$ . The diameter value for  $H_0$  is about 50 percent and the magnitude value about 30 percent larger than those obtained from the direct relation (cf. Theureau et al. 1997b).
2. We examined whether this discrepancy could be resolved in terms of some selection effect in  $\log V_{\text{max}}$  and the type dependence of the zero-points on the Hubble type. One expects these to have some influence on the derived value of  $H_0$ . Only a minuscule effect was observed.
3. There is – however – a new kind of bias involved: if the  $\log V_{\text{max}}$ -distribution of the calibrators does not reflect the cosmic distribution of the field sample *and* the relevant slope for the field galaxies differs from the calibrator slope the average value of  $\log H_0$  will be biased if the relevant slope is used (Teerikorpi et al. 1999).
4. We showed for the unbiased inverse plateau galaxies i.e. a sample without galaxies probably suffering from selection in  $\log V_{\text{max}}$ , that the calibrators and the field sample obey

different inverse diameter slopes, namely  $a'_{\text{cal}} = 0.73$  and  $a' = 0.54$ . Also, the magnitude slopes differed from each other ( $a'_{\text{cal}} = -0.147$  and  $a' = -0.115$ ). For the diameter relation we were able to use 2142 galaxies and for the magnitude relation 1713 galaxies. These sizes are significant.

5. We also found evidence that the calibrator sample does *not* follow the cosmic distribution of  $\log V_{\text{max}}$  for the field galaxies. This means that if the relevant slopes are used a too large value for  $H_0$  is found. Formally, this calibrator selection bias could be corrected for but is a complicated task.
6. One may use instead of the relevant slope the calibrator slope which also brings about a biased value of  $H_0$ . Now, however, the correction for the bias is an easy task. Furthermore, this approach can be used irrespective of the nature of the calibrator sample and should yield an unbiased estimate for  $H_0$ .
7. When we adopted this line of approach we found
  - $H_0 = 52^{+5}_{-4} \text{ km s}^{-1} \text{ Mpc}^{-1}$  for the inverse diameter B-band Tully-Fisher relation, and
  - $H_0 = 53^{+6}_{-5} \text{ km s}^{-1} \text{ Mpc}^{-1}$  for the inverse magnitude B-band Tully-Fisher relation
 for a strictly homogeneous distribution of galaxies ( $\alpha = 0$ ) and
  - $H_0 = 59^{+5}_{-4} \text{ km s}^{-1} \text{ Mpc}^{-1}$  for the inverse diameter B-band Tully-Fisher relation, and
  - $H_0 = 58^{+6}_{-5} \text{ km s}^{-1} \text{ Mpc}^{-1}$  for the inverse magnitude B-band Tully-Fisher relation.
 for a decreasing radial density gradient ( $\alpha = 0.8$ ).

These values are in good concordance with each other as well as with the values established from the corresponding direct Tully-Fisher relations derived by Theureau et al. (1997b), who gave a strong case for the long cosmological distance scale consistently supported by Sandage et al. (1995). Our analysis also establishes a case supporting such a scale. It is worth noting that this is the first time when the *inverse* Tully-Fisher relation clearly lends credence to small values of the Hubble constant  $H_0$ .

*Acknowledgements.* We have made use of data from the Lyon-Meudon extragalactic Database (LEDA) compiled by the LEDA team at the CRAL-Observatoire de Lyon (France). This work has been supported by the Academy of Finland (projects ‘‘Cosmology in the Local Galaxy Universe’’ and ‘‘Galaxy streams and structures in the Local Universe’’). T. E. would like to thank G. Paturel and his staff for hospitality during his stay at the Observatory of Lyon in May 1998. Finally, we thank the referee for useful comments and constructive criticism.

## Appendix A: the relevant slope and an unbiased $H_0$

In this appendix we in simple manner demonstrate how the relevant slope introduced in Sect. 2.2 indeed is the slope to be used. Consider

$$\log H_0 = \log V_{\text{cor}} - \log R_{\text{iTF}}, \quad (\text{A1})$$

where the velocity corrected for the peculiar motions,  $V_{\text{cor}}$ , depends on the relative kinematical distance scale as

$$\log V_{\text{cor}} = \log C_1 + \log d_{\text{kin}} \quad (\text{A2})$$

and the inverse Tully-Fisher distance in Mpc is<sup>2</sup>

$$\log R_{\text{iTF}} = Ap + B_{\text{cal}} - x + \beta \quad (\text{A3})$$

The constant  $C_1$  was defined by Eq. 11 and can be decomposed into  $\log C_1 = \log H_0^* + \log C_2$ .  $H_0^*$  is the true value of the Hubble constant and  $C_2$  transforms the relative distance scale into the absolute one:  $\log R_{\text{kin}} = \log d_{\text{kin}} + \log C_2$ . Because  $X_{\text{kin}} = \log R_{\text{kin}} + x - \beta$  Eq. A1 reads:

$$\log H_0 - \log H_0^* = X_{\text{kin}} - Ap - B_{\text{cal}}. \quad (\text{A4})$$

Consider now a subsample of galaxies at a constant  $X_o$ . By realizing that  $X_{\text{kin}} = X_o + (B' - B_{\text{in}})$ , where  $B'$  gives the true distance scale and  $B_{\text{in}}$  depends on the adopted distance scale (based on the input  $H_0$ ), and by taking the average over  $X_o$  Eq. A4 yields

$$\langle \log H_0 \rangle_{X_o} - \log H_0^* = X_{\text{kin}} - A\langle p \rangle_{X_o} - B_{\text{cal}}. \quad (\text{A5})$$

The use of  $B'$  is based on two presumptions, namely that the underlying kinematical model indeed brings about the correct relative distance scale and that the adopted value for  $C_1$  genuinely reflects the true absolute distance scale. If the adopted slope  $a'_o$  is the relevant one we find using Eq. 19  $A\langle p \rangle_{X_o} = X_o - B_{\text{in}}$  and

$$\langle \log H_0 \rangle_{X_o} - \log H_0^* = (B' - B_{\text{in}}) - (B_{\text{cal}} - B_{\text{in}}). \quad (\text{A6})$$

As a final result we find

$$\langle \log H_0 \rangle_{X_o} - \log H_0^* = (b'_{\text{cal}} - b'_{\text{true}})/a'_o. \quad (\text{A7})$$

Because Eq. A7 is valid for each  $X_o$ , the use of the relevant slope necessarily guarantees a horizontal run for  $\langle \log H_0 \rangle$  as a function of  $X_o$ .

## Appendix B: note on a theoretical diameter slope $a' \sim 0.75$

Theureau et al. (1997a) presented theoretical arguments which supported the inverse slope  $a' = 0.5$  being derived from the field galaxies. Consider a pure rotating disk (the Hubble type 8). The square of the rotational velocity measured at the radius  $r_{\text{max}}$  at which the rotation has its maximum is directly proportional to the mass within  $r_{\text{max}}$ , which in turn is proportional to the square of  $r_{\text{max}}$ . Hence,  $\log V_{\text{max}} \propto 0.5 \log r_{\text{max}}$ . By adding a bulge with a mass-to-luminosity ratio differing from that of the disk, and a dark halo with mass proportional to the luminous mass, one can as a first approximation understand the dependence of the zero-point of the inverse relation on the Hubble type.

However, the present study seems to require that the theoretical slope  $a'$  is closer to 0.75 rather than 0.5. The question

<sup>2</sup> The numerical constant  $\beta = 1.536274$  connects  $x$  in 0.1 arcsecs,  $X$  in kpc and  $R_{\text{iTF}}$  in Mpc

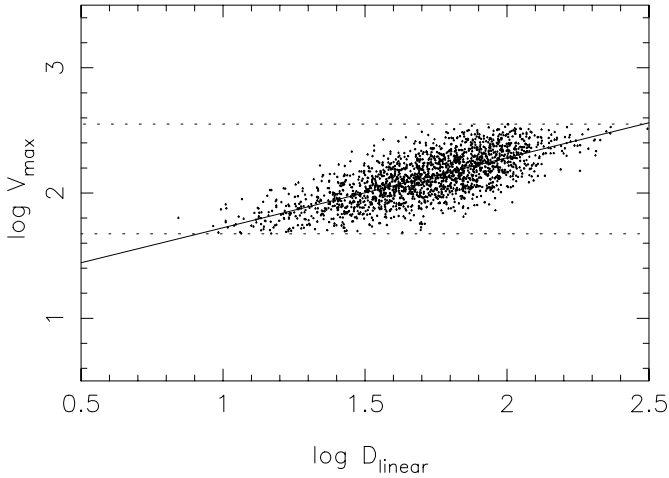


**Fig. C1.** A synthetic Virgo supercluster subjected to a bias caused by measurement errors in apparent diameters and upper and lower cut-offs in  $\log V_{\max}$ .

arises whether the simple model used by Theureau et al. (1997a) could in some natural way be revised in order to produce a steeper slope. In fact, the model assumed that for each Hubble type the mass-to-luminosity ratio  $M/L$  is constant in galaxies of different sizes (luminosities). If one allows  $M/L$  to depend on luminosity, the slope  $a'$  will differ from 0.5. Especially, if  $M/L \propto L^{0.25}$ , one may show that the model predicts the inverse slope  $a' = 0.75$ . The required luminosity dependence of  $M/L$  is interestingly similar to that of the fundamental plane for elliptical galaxies and bulges (Burstein et al. 1997). The questions of the slope, the mass-to-luminosity ratio and type-dependence will be investigated elsewhere by Hanski & Teerikorpi (1999, in preparation).

### Appendix C: how to explain $a'_{\text{obs}} < a'$ ?

Among other things ET97 discussed how a gaussian measurement error  $\sigma_x$  in apparent diameters yields a too large value for  $H_0$ . How does the combination of cut-offs in  $\log V_{\max}$  - distribution and this bias affect the slope? We examined this problem by using a synthetic Virgo Supercluster (cf. Ekholm 1996). As a luminosity function we chose

$$\log D = 0.28 \times G(0, 1) + 1.2 \quad (\text{C1})$$

and as the inverse relation

$$\log V_{\max} = 0.11 \times G(0, 1) + a'_t \log D + 0.9, \quad (\text{C2})$$

where  $G(0, 1)$  refers to a normalized gaussian random variable. As the “true” inverse slope we used  $a'_t = 0.75$ . The other numerical values were adjusted in order to have a superficial resemblance with Fig. 5. We first subjected the synthetic sam-

ple to the upper and lower cut-offs in  $\log V_{\max}$  given in Sect. 4. The resulting slope was  $a' = 0.692$ . A dispersion of  $\sigma_x = 0.05$  yielded  $a' = 0.642$  and  $\sigma_x = 0.1$   $a' = 0.559$ . The inverse Tully-Fisher diagram for the latter case is shown in Fig. C1. Though the model for the errors is rather simplistic this experiment shows a natural way of flattening the observed slope  $a'$  with respect to the input slope  $a'_t$ .

### References

- Bottinelli L., Gouguenheim L., Paturel G., Teerikorpi P., 1986, A&A 156, 157
- Branch D., 1998, ARA&A 36, 17
- Burstein D., Bender R., Faber S.M., Nolthenius R., 1997, AJ 114, 1365
- Cen R., 1998, ApJ 498, L99
- Cooray A., 1998, A&A 339, 623
- Di Nella H., Montuori M., Paturel G., et al., 1996, A&A 308, L33
- Eisenstein D., Hu W., Tegmark M., 1998, ApJ 504, L57
- Ekholm T., Teerikorpi P., 1994, A&A 284, 369
- Ekholm T., 1996, A&A 308, 7
- Ekholm T., Teerikorpi P., 1997, A&A 325, 33 (ET97)
- Federspiel M., Sandage A., Tammann G.A., 1994, ApJ 430, 29
- Federspiel M., Tammann G.A., Sandage A., 1998, ApJ 495, 115
- Fouqué P., Bottinelli L., Gouguenheim L., Paturel G., 1990, ApJ 349, 1
- Freudling W., da Costa L.N., Wegner G., et al., 1995, AJ 110, 920
- Giovanelli R., Hayes M., da Costa L., et al., 1997, ApJ 477, L1
- Gouguenheim L., 1969, A&A 3, 281
- Hendry M.A., Simmons J.F.L., 1994, ApJ 435, 515
- Hughes J., Birkinshaw M., 1998, ApJ 501, 1
- Jensen J., Tonry J., Colley W., et al., 1999, ApJ 510, 71
- Kundić T., Turner E., Colley W., et al., 1997, ApJ 482, 75
- Paturel G., Di Nella H., Bottinelli L., et al., 1994, A&A 289, 711
- Paturel G., Lanoix P., Teerikorpi P., et al., 1998, A&A 339, 671
- Peebles P.J., 1976, ApJ 205, 318
- Rauzy S., Triay R., 1996, A&A 307, 726
- Riess A., Filippenko A., Challis P., et al., 1998, AJ 116, 1009
- Salaris M., Cassisi S., 1998, MNRAS 298, 166
- Sandage A., 1994a, ApJ 430, 1
- Sandage A., 1994b, ApJ 430, 13
- Sandage A., Tammann G.A., Federspiel M., 1995, ApJ 452, 1
- Schechter P.L., 1980, AJ 85, 801
- Teerikorpi P., 1984, A&A 141, 407
- Teerikorpi P., 1990, A&A 234, 1
- Teerikorpi P., 1993, A&A 280, 443
- Teerikorpi P., 1997, ARA&A 35, 101
- Teerikorpi P., Hanski M., Theureau G., et al., 1998, A&A 334, 395
- Teerikorpi P., Ekholm T., Hanski M., Theureau G., 1999, A&A 343, 713
- Theureau G., Hanski M., Teerikorpi P., et al., 1997a, A&A 319, 435
- Theureau G., Hanski M., Ekholm T., et al., 1997b, A&A 322, 730
- Theureau G., Bottinelli L., Coudreau-Durand N., et al., 1998, A&AS 130, 333
- Tully R.B., Fisher J.R., 1977, A&A 54, 661
- Willick J.A., 1991, Ph.D. Thesis, University of California, Berkeley